Ecotoxicology (2026) 35:77
https://doi.org/10.1007/s10646-026-03066-z

Photosynthetic modulation and oxidative stress in *Raphidocelis subcapitata* exposed to environmentally relevant concentrations of a ketoconazole based commercial formulation

Caio César Achiles do Prado[1,3] · Lucas Gonçalves Queiroz[2] · Flávio Teixeira da Silva[3] · Teresa Cristina Brazil de Paiva[4]

Received: 24 September 2025 / Accepted: 5 March 2026 / Published online: 18 March 2026
© The Author(s) 2026

Abstract

Antifungal drugs such as ketoconazole (KTZ) are increasingly detected in aquatic environments, raising concerns about their potential ecotoxicological effects on non-target organisms. In this study, we evaluated the physiological, biochemical, and morphological responses of the freshwater microalga *Raphidocelis subcapitata* exposed to environmentally relevant concentrations of KTZ. Initially, based on chronic exposure analyses, toxicity was observed at concentrations ≥ 1.9 µg/L, and the IC_{50} value was 7.2 µg/L after 120 h of exposure. Subsequently, assays using sub-inhibitory concentrations (2.8 and 5.6 µg L^{-1}) were conducted for 96 h and 192 h to evaluate selected endpoints, including changes in growth rate, photosynthetic pigments, cell morphology, lipid production, and oxidative stress, with exposure duration influencing these responses. These findings revealed a dual nature of KTZ toxicity: while low concentrations may stimulate photosynthetic activity, higher levels trigger oxidative stress. In addition, exposure time also influenced the effects observed in *R. subcapitata*. Our results underscore the importance of multivariate approaches in ecotoxicology and contribute to a deeper understanding of the environmental risks associated with pharmaceutical contaminants in freshwater ecosystems.

Keywords azole fungicides · ketoconazole · chlorophyte algae · growth inhibition · oxidative stress

✉ Caio César Achiles do Prado
ccaprado@unifesp.br; caioachiles@gmail.com

Lucas Gonçalves Queiroz
queiroz@ib.usp.br

Flávio Teixeira da Silva
flaviots@usp.br

Teresa Cristina Brazil de Paiva
teresapaiva@usp.br

1 Sea Institute, Department of Marine Sciences, Federal University of São Paulo (Unifesp), Dona Maria Máximo Street 168, Santos 11070-100, Brazil

2 Department of Clinical and Toxicological Analyses, School of Pharmaceutical Sciences, University of São Paulo, Professor Lineu Prestes Avenue 580, São Paulo 05508-000, Brazil

3 Department of Biotechnology, Engineering School of Lorena, University of São Paulo (EEL/USP), Municipal do Campinho Road, Lorena 12602-810, Brazil

4 Department of Basic and Environmental Sciences, Engineering School of Lorena, University of São Paulo (EEL/USP), Municipal do Campinho Road, Lorena 12602-810, Brazil

Introduction

The largest class of synthetic antifungal agents, the azole compounds, has been detected in aquatic environments worldwide. Over recent decades, there has been a noticeable rise in the use and demand for these molecules, with the United States alone producing an average of around 300,000 tons per year (Bhagat et al. 2021). Recent studies have provided comprehensive summaries on the prevalence and environmental fate of azole compounds in aquatic ecosystems, as well as their potential ecological risks to biota (Assress et al. 2020; Wroński et al. 2024; Iancu et al. 2024). An example of an azole contaminant is ketoconazole (KTZ), which is an imidazole antifungal with broad spectrum and systemic action, launched in 1981 by the Belgian company Janssen Pharmaceuticals (Shafiei et al. 2020). This drug exerts its antifungal activity by inhibiting lanosterol 14α-demethylase, thereby disrupting ergosterol biosynthesis and directly compromising fungal cell membrane integrity, viability, and growth (Sadozai et al. 2020).

KTZ has been detected across various aquatic environmental matrices. In sewage treatment plants (STPs), azole compound concentrations have been reported to range from 6.7 ng/L to 1.1 µg/L in effluent (Assress et al. 2020; Maraqa et al. 2020; Wattanayon et al. 2023),, and 0.37 µg/L to 143 µg/L in influent samples (Maraqa et al. 2020; Skalska-Tuomi et al. 2025). Additionally, KTZ has been identified in multiple environmental compartments, with concentrations in surface water ranging from 0.6 ng/L to 1.3 µg/L(Bhagat et al. 2021; Dehm et al. 2021; Wroński et al. 2024) and in sediment from 5 ng/g to 5.2 µg/g (Peng et al. 2012; Chaves et al. 2020; Bhagat et al. 2021; Wroński et al. 2024). In the study byStyszko et al. (2025), even after primary and secondary treatments, the residual concentration of KTZ in stabilized sludge samples exceeding 100 mg/kg indicates the persistence of this compound in the environment. The relatively low concentrations of ketoconazole detected in surface waters may be partially explained by its physicochemical properties. The low pKa values of KTZ (2.9 and 6.5) indicate that it is a weakly basic compound, a diprotic base that can protonate both the imidazole ring and the piperazine moiety under acidic conditions (Hussain et al. 2021). Thus, KTZ exhibits pH-dependent solubility, and acid–base behavior enhances its affinity for hydrophobic matrices, thereby promoting adsorption to sediments (Styszko et al. 2025) and interactions with biological membranes (Hussain et al. 2021).

From an environmental perspective, the presence of these compounds in the environment may pose risks to aquatic environments, especially for non-target organisms (Batucan et al. 2022). In previous studies carried out with macroinvertebrates, it was observed that exposure to KTZ for 48 h promoted toxic effects on *Daphnia similis* (EC_{50} = 4.3 µg/L) and *Chironomus sancticaroli* (LC_{50} = 9.9 µg/L). In addition, changes in oxidative stress biomarkers were also observed by Prado et al. (2023, 2021). KTZ not only inhibits CYP enzymes but may also impact the endocrine functions of organisms, as observed in daphnids (Hannas et al. 2011; Prado et al. 2021).

However, few studies have reported chronic and/or sublethal effects of KTZ on photosynthetic organisms such as green microalgae (Chen and Ying 2015; Yousefi-Ahmadipour et al. 2016; Villain et al. 2016; Yamagishi et al. 2017). In particular, no published studies have investigated prolonged exposures to KTZ using environmentally relevant concentrations. Consequently, impacts that affect the base of the food chain, including periphyton, phytoplankton, and zooplankton, have the potential to cause significant harm to aquatic communities, compromising both their stability and ecological functions (Guo et al. 2020; Bhagat et al. 2021; Qin et al. 2024; Yang et al. 2025). Therefore, further studies are needed to understand how KTZ affects the base of the freshwater food chain.

Many studies have used the species *Raphidocelis subcapitata* (synonym of *Pseudokirchneriella subcapitata*) as an indicator organism of environmental quality, which is widely used in ecotoxicological tests of xenobiotics (OECD 2011; ABNT 2018). The literature demonstrates that the inhibition of ergosterol biosynthesis caused by KTZ can directly impact the functioning of *R. subcapitata* (Villain et al. 2016; Yamagishi et al. 2017). In addition, studies show that contact with azole compounds can cause changes in biochemical responses in chlorophyte algae, triggering changes in photosynthetic capacity and redox response (Nong et al. 2021).

The absence of information on KTZ's impacts on these species underscores a significant knowledge gap about how the chronic effects of this antifungal drug influence biological mechanisms. Furthermore, the few studies available in the literature have focused solely on the active compound, with no investigations addressing commercial formulations, which may significantly influence the toxicological responses of non-target organisms. In this context, the present study aimed to expand knowledge on the effects of environmental concentrations of a commercial KTZ formulation on aquatic ecosystems by investigating the multiple effects of this antifungal drug on the growth, chlorophyll content, lipid storage, oxidative stress, and morphological development of *R. subcapitata.*

Materials and methods

Chemical

In the present study, a commercial ketoconazole KTZ) formulation was selected to assess the effects of both the active ingredient and the excipients present in the pharmaceutical product. Therefore, the commercial formulation of KTZ used in the present study was acquired locally (Neo Quimica, 10 tablets, 200 mg). KTZ calibration curve was constructed using the pharmaceutical secondary standards for application in quality control (Sigma-Aldrich, certified reference material CAS number: 65277-42-1). HCl (99.9%, HPLC grade, Sigma-Aldrich) was used to dilute the calibration curve. Methanol (99.9%, HPLC grade, J.T. Baker, Fisher Scientific) was used as the solvent for KTZ commercial formulation, yielding a theoretical concentration of 4 g/L.

KTZ curve calibration

To confirm the stock solution concentration, the KTZ was quantified by ultraviolet absorption spectrophotometry (λ = 223 nm) following the methodology of Rubim et al. (2012). The standard curve for analytical drug quantification was performed, requiring a correlation coefficient ($_{\rho}$) of at least 0.999 to validate the quantification. A stock solution was prepared by dissolving 25 mg of commercial KTZ in 250 mL of methanol. After homogenization, 2 mL of the solution was filtered (7.5 µm porosity) and diluted to 50 mL with 0.1 M HCl to obtain a 4.0 µg/mL solution. Calibration was performed using KTZ solutions at 0, 100, 200, 300, 400, 500, and 600 µg/mL. Absorbance was measured at 223 nm with 0.1 M HCl as the blank (Figure S1).

Cultivation and maintenance of organisms

Algae were cultured in LC Oligo medium at 25 ± 2 °C, with a light intensity of 4500 lx, in a shaker incubator with continuous agitation at 150 rpm, following the protocol proposed by ABNT NBR 12,648/18 (ABNT 2018), similar to the OECD guideline 201 (OECD 2011). The cultivation and toxicity testing conditions for *R. subcapitata* described in ABNT NBR 12,648 are largely consistent with those established by OECD guideline 201, differing mainly in minor operational aspects and regulatory scope, while maintaining equivalent endpoints, environmental conditions, and validation criteria. The inoculum was transferred during the exponential growth phase, between 96 and 120 h, at an initial concentration of approximately 10^5 cells/mL in 100 mL of culture medium. Cell counts were performed in a Neubauer chamber under optical microscopy, and the experiment was performed in triplicate. Periodically, sensitivity analyses were performed using zinc sulfate ($ZnSO_4.7H_2O$) as a reference substance. The sensitivity ranges were determined by calculating the effective concentration that inhibited 50% of the algal biomass (IC_{50}) after 120 h of exposure, under the same laboratory conditions (Figure S2).

Growth inhibition rate

The algae in the exponential growth phase (10^5 cells/mL) were used for exposure to the KTZ drug. The tests were performed exposing the algae to different KTZ concentrations (0.0, 1.9, 3.9, 7.8, 15.6, 31.2, 62.5, 125, 250, 500, and 1000 µg/L) for 120 h at 25 ± 2 °C, 4500 lx, and 150 rpm. Assays were performed in triplicate, using 250 mL Erlenmeyer flasks containing 100 mL of test solution. At the end of the exposure period, 1 mL of lugol solution was added to inhibit algal growth, and then the count was performed. The results were validated when, at the end of the test, the algal density of the control treatment was at least 100 times higher than the initial density, with a coefficient of variation less than or equal to 20%. The growth inhibition rate in percentage (IC_{50}) for each KTZ concentration evaluated was calculated compared to the control. Growth inhibition tests were performed based on established methodology (ABNT 2018).

Subinhibitory effects

For investigation of subinhibitory effects, two effect concentrations (below IC_{50}) were selected for exposure of 192 h (IC_{20} = 5.6 µg/L and IC_{10} = 2.8 µg/L). The selected concentrations are environmentally relevant, considering recent studies that detected KTZ in wastewaters and aquatic systems in concentrations varying from 1 to 143 µg/L (Maraqa et al. 2020; Wroński et al. 2024). The conditions for the growth inhibition test were identical to those for the algal culture. The microalgal suspension was collected at regular time points (0, 96, and 192 h) to measure cell density. Sampling points were selected based on the growth kinetics curve, with sampling conducted at the initial stage (0 h), during the logarithmic growth phase (96 h), and at the final stage (192 h) (Figure S3). Additionally, the pH of the cultures was measured at each aliquot sampling.

Photosynthetic pigments

Aliquots of 3 mL of microalgal suspension were withdrawn from each flask every 48 h and stored at -20 °C under refrigeration until analysis was carried out. The stored samples were filtered through glass membrane filters (1.2 µm). Then, the filter was placed in a 15 mL conical tube with 3 mL of 90% acetone, slightly homogenized, macerated with a glass stick, and stored under refrigeration (-20 °C) for 24 h. Subsequently, the tubes were centrifuged at 4000 rpm for 15 min at 20 °C. The resulting supernatant was analyzed by a spectrophotometer at 470, 653, 664, and 666 nm. For the reading blank, 90% acetone was used. The levels of photosynthetic pigments, chlorophyll a, b, and total carotenoids, were determined as demonstrated by Guo et al. (2020) and expressed in mg/L.

Total lipids (Bligh-Dyer method)

After 120 h, 30 mL of microalgal suspension was withdrawn from each flask, placed in 50 mL centrifuge tubes, and centrifuged at 4000 g for 15 min. For extraction, each 100 mg of algal biomass was mixed with: 500 µL of methanol (shaken for 2 min), 125 µL of chloroform (shaken for 5 min), 125 µL of chloroform (shaken for 2 min), 200 µL of distilled H_2O (shaken for 5 min), and centrifuged at

4000 g for 10 min at 20 °C. Subsequently, the biomass was resuspended in 200 µL of chloroform, stirred for 5 min, and centrifuged at 4000 g for 10 min at 20 °C. The supernatant was collected and stored; this was repeated three times. In the end, all collected supernatant was pooled, added to an already tared container, and dried in an oven at 105 °C until stabilization (Jesus et al. 2019). The analysis was performed in triplicate. The lipid content was calculated by dividing the initial weight by the final weight after drying. The algal biomass wet weight was used to normalize the results. Additionally, cells were imaged by fluorescence microscopy to analyze lipid storage, as proposed by Priyanka et al. (2020). Nile Red dye (0.3 mg/mL, diluted in acetone) was added to the cell suspension at a ratio of 1:1.5 and incubated at 40 °C for 1 h. Subsequently, slides were prepared in triplicate, and a drop of algal suspension was added, followed by a coverslip. The slides were evaluated using fluorescence microscopy, with an Olympus BX53 model equipped with an X-CITE 120 LED source, a U-FGW filter, and an excitation wavelength of 530–550 nm and an emission wavelength of 575 nm. The images were captured, measured, and processed using CellSens 8.0 Software. The exposure time was standardized to 40 ms for all treatments. For each slide, 100 cell units were counted, and then cell volume (μm^3) and cell length (µm) were evaluated.

Oxidative stress biomarkers

Aliquots (10 mL) were taken out after subinhibitory exposure to KTZ for 0, 96, and 192 h. Then, the sample was centrifuged at 4000 rpm for 10 min and stored at -20 °C. The exact process was carried out with the inoculum to start the test and obtain the initial time values. Frozen biomass samples (-80 °C) were processed using 1 mL of potassium phosphate buffer (100 mM, pH 7.4) and manually macerated with a quartz mortar and pestle for 3 min. The entire process was carried out in an ice bath to ensure the sample integrity. Then, the homogenate was centrifuged at 4000 g for 30 min at 4 °C. The resulting supernatant was used to analyze oxidative stress biomarkers. The results were normalized to the homogenate's protein content.

Lipid peroxidation (LPO) LPO was evaluated by thiobarbituric acid reactive substances (TBARS) assay, which measures malondialdehyde (MDA) production as described by Prado et al. (2023) with modifications. The assay was performed using 0.4% thiobarbituric acid (TBA) in 100 mM potassium phosphate buffer (pH 2.5). In 2 mL microtubes, 500 µL of homogenate and 1 mL of TBA solution were added, and the mixture was thoroughly homogenized. The reaction mixtures were incubated in a water bath at 95 ± 2 °C for 45 min and then immediately cooled in an ice bath to terminate the reaction. After cooling, samples were centrifuged at 3,000 rpm for 5 min at 25 °C, and the absorbance of the supernatant was measured at 532 nm. Blank samples consisted of 500 µL of potassium phosphate buffer (100 mM, pH 7.4) mixed with 1000 µL of 0.4% TBA. Standard controls were prepared following the same procedure, replacing the buffer with 4.5 mM 1,1,3,3-tetraethoxypropane (TEP) LPO was expressed by nmol MDA/mL.

Catalase (CAT) CAT activity was determined as described by (Prado et al., 2021). The assays were conducted in 100 mM potassium phosphate buffer (pH 7.0) containing 20.0 mM hydrogen peroxide (H_2O_2) at a 1:1 (v/v) ratio, using 20.0 µL of homogenate. Enzyme activity was monitored by measuring the decrease in absorbance at 240 nm over a 3 min period, corresponding to H_2O_2 consumption. CAT activity was defined as the amount of enzyme required to decompose 1 µmol of H_2O_2/min/mg protein.

Superoxide dismutase (SOD) SOD activity was determined as described by Prado et al. (2023). In 2 mL microtubes, 1.3 mL of tris-EDTA buffer (5 mM, pH 8.0), 60 µL of the sample, and 75 µL of pyrogallic acid solution (15 mM) were added, and the mixture was homogenized. Assays were incubated for 30 min in the dark at 25 °C. After incubation, the oxidation reaction was stopped by adding 65 µL of 1 N HCl. The same preparation was performed for the blank, using 60 µL of 100 mM potassium phosphate buffer (pH 7.4). SOD activity was determined by the ability to inhibit the oxidation of 50% pyrogallol and expressed as µmol SOD/min/mg protein.

Glutathione S-transferase (GST) GST activity was determined as described by Prado et al. (2023). The assays were carried out in triplicate, with 490 µL of 100 mM potassium phosphate buffer (pH 6.5) added, 490 µL of the mix solution (9.5 mM reduced glutathione (GSH) /1-chloro-2,4-Dinitrobenzene (CDNB) 1.0 mM, diluted in 100 mM potassium phosphate buffer (pH 6.5) and methanol, respectively) and 20 µl of homogenate. The same solution was prepared for the blank, using the buffer. GST activity was monitored by measuring the increase in absorbance at 340 nm for 5 min after forming the S- (2,4-dinitrophenyl) conjugate of glutathione and expressed as µmol CDNB-GSH/min/mg protein.

Ascorbate peroxidase (APx) APX activity was measured by Prado et al. (2021). Assays were conducted using potassium phosphate buffer 100 mM (pH 7.5), ascorbic acid 0.5

mM, hydrogen peroxide 0.1 mM, and 20.0 µL of the sample solution. The activity was determined by measuring the decrease in absorbance at 290 nm due to the consumption of ascorbate (AsA) over 2 min. APX activity is defined as the consumption of 1 µmol of ASC/min/mg protein.

Protein Protein concentration was determined according to the Bradford (1976) method. A standard protein curve was prepared using bovine serum albumin (BSA) at 100 mg/mL in 100 mM potassium phosphate buffer, pH 7.5. Serial dilutions were then performed to obtain concentrations ranging from 0 to 62.5 µg mL-1 in a volume of 20 µL.

Statistical analysis

Data were reported as mean ± standard deviations (SD). Probit analysis was used to estimate the concentration-response relationship for the toxicity of KTZ exposure. All data were subjected to Shapiro-Wilk normality tests and homogeneity of variance (Levene test) with a significance level of 95% ($p < 0.05$). Toxicological parameters (inhibition, growth, biochemical) were analyzed for statistical differences using one-way ANOVA, followed by Fisher's LSD and Dunnett's test. Principal component analysis (PCA) is used to analyze the interactions among the observed variables. The analyses were processed using OriginPro® 2025 and GraphPad Prism 8.0 for graph construction and statistical analysis. All analyses were conducted with a significance level $\alpha = 0.05$.

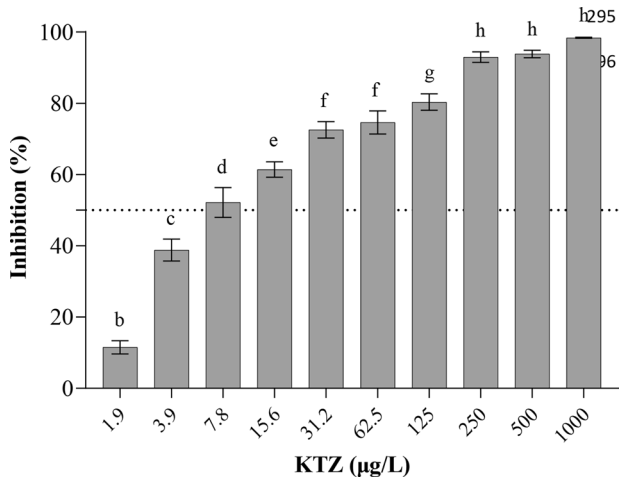


Fig. 1 Chronic toxicological parameter of KTZ in *R. subcapitata* after 120 h. The inhibition rate was normalized to 100% in the control group (without KTZ). The dashed line represents the median inhibitory concentration (IC_{50}). The letters represent the averages of the treatments; equal letters indicate equal averages, whereas different letters denote differences between them

Results and discussion

Growth inhibition

Assays with *R. subcapitata* demonstrated inhibition of algal growth at high concentrations of KTZ, with inhibition exceeding 80% at 125 µg/L of KTZ (Fig. 1). Additionally, the IC_{50} was determined to be 7.2 µg/L (6.6–7.7 µg/L). After 120 h of exposure, all testes KTZ concentrations showed a significant difference compared to the control group ($p < 0.05$). No toxic effects were observed in the methanolic control, even at the highest concentrations tested (Table S1), indicating that the progressive inhibition observed in the assays was attributable to increasing KTZ levels rather than to methanol.

Studies already demonstrate the toxicological potential of KTZ on *R. subcapitata*. Yamagishi et al. (2017) observed growth inhibition in *R. subcapitata* after 72 h of exposure, showing toxicity from 0.28 mg/L and an IC_{50} of 1.72 mg/L (values calculated from molarity). Likewise, Chen and Ying (2015) identified KTZ toxicity after 96 h of exposure (IC_{50} 4.3 mg/L), and showed chronic toxicity from 1.8 mg/L. Villain et al. (2016) and Yousefi-Ahmadipour et al. (2016) observed toxicity (EC_{50}) for *R. subcapitata* after 72 h, of 2.8 mg/L and 0.3 mg/L of KTZ, respectively. Using a commercial KTZ, we observed higher toxicity than reported in the literature. Studies suggest that the toxicity of commercial compounds may be attributed to the presence of excipients, increasing the degree of their toxicity (Grycová et al. 2015; Prado et al. 2021, 2023).

In addition to KTZ, other azole compounds have also been shown to be toxic to chlorophyll algae. Chen et al. (2014) observed toxicity of fluconazole (a triazole fungicide) in *R. subcapitata* at 4.5 mg/L. Pan et al. (2018) observed the inhibition of algal growth of *Scenedesmus obliquus* with 2 mg/L of climbazole (triazole fungicide). Studies performed with metronidazole (an imidazole antibiotic and antiprotozoal) showed IC_{50} for *Chlorella* sp. and *R. subcapitata* at 12.5 and 40.4 mg/L, respectively (Fu et al. 2017). However, the same compound (metronidazole) showed greater toxicity to *Desmodesmus* and *Scenedesmus* species, with IC_{50} ranging from 7.8 to 125 µg/L (Miazek and Brozek-Pluska 2019). Morais et al. (2014) reported an IC_{50} value of 98 µg/L for clotrimazole (an imidazole fungicide) in *R. subcapitata*. However, Gonçalves et al. (2021) determined higher toxicity for clotrimazole, with an IC_{50} of 0.15 mg/L. Del Puerto et al. (2022) observed the toxicity of tebuconazole (triazole fungicide) at 12.2 mg/L. Furthermore, we observed that imidazole compounds, as the literature has shown, are more toxic to Chlorophyceae microalgae than triazole compounds.

Subinhibitory effects of KTZ on *R. subcapitata*

Growth, morphology, and lipid production

Several parameters can be used to evaluate toxic effects on microalgae. The growth kinetics of *R. subcapitata* showed inhibition of 12% and 25% after 192 h of exposure to KTZ at concentrations of 2.8 and 5.6 µg/L, respectively (Table 1). The present study observed that microalgae exposed to KTZ underwent significant changes in size and biochemical responses after 192 h (Table 1) only at the highest concentration.

A decrease of 1.9 μm^3 in cell volume and 0.9 µm in cell length was observed for the 5.6 µg/L compared with the control treatment (Table 1). Additionally, protein levels were affected by KTZ, with mean reductions of 4% and 30% at concentrations of 2.8 µg/L and 5.6 µg/L, respectively (Table 1). Thus, the most sensitive responses were observed for the lipid and protein content endpoints, even at the lowest concentration tested. We believe that this response is associated with prolonged exposure, even at low concentrations, which is sufficient to affect organism physiology. This effect is possibly related to increased oxidative damage to cellular structures, as previously reported in studies evaluating azole compounds in *R. subcapitata* (Huang et al. 2025).

Nong et al. (2021) observed a decrease in protein levels in *Chlorella pyrenoidosa* after exposure to three azole compounds, myclobutanil (≤20 mg/L), propiconazole (≤2 mg/L), and tebuconazole (≤1 mg/L) for 96 h. A similar response was reported by Qin et al. (2024), when exposing *Auxenochlorella pyrenoidosa* to cyproconazole (1.53 mg/L, a triazole fungicide), imazalil (3.98 mg/L, an imidazole fungicide), and prochloraz (0.78 mg/L, an imidazole fungicide) for 96 h. It is essential to note that protein content is closely linked to cell density and, consequently, to cell growth, as shown in Table 1. The reduction in lipid production in *R. subcapitata* was approximately 53% and 68% at 2.8 µg/L and 5.6 µg/L, respectively (Table 1). Using fluorescence microscopy, we observed a decrease in lipid content in *R. subcapitata* (Fig.2).

Many algae have as an energy reserve the storage of carbohydrates and lipids in their cells, such as *R. subcapitata* (Liu et al. 2019). As is already known, imidazole compounds such as KTZ directly inhibits ergosterol production in microalgae (Yamagishi et al. 2017). It is widely understood that green algae produce ergosterol as a component of their cell membranes and biological activities (Volkman 2003; Yamagishi et al. 2017). Voshall et al. (2021) observed inhibition of ergosterol biosynthesis of 47–57% for *Chlorella sorokiniana* and 38–44% for *Chlorella variabilis* after exposure to clotrimazole and KTZ, respectively. A 64% reduction in total sterol production was observed by Porsbring et al. (2009) in marine algal communities exposed to 0.172 µg/L (values calculated from molarity) of clotrimazole after 96 h. Thus, we hypothesize that the reduction in lipid levels in *R. subcapitata* may be attributable to the inhibitory effects of KTZ, which may indirectly affect the organism's growth rate.

Table 1 Biochemical and morphological parameters of *R. subcapitata* after exposure to commercial KTZ (192 h)

Parameters	KTZ (µg/L)		
	0	2.8	5.6
Lipid (mg/100 mg)	7.2 ± 0.5^a	3.3 ± 0.2^b	2.3 ± 0.5^b
Protein (µg/mL)	39.2 ± 0.5^a	37.6 ± 0.2^b	27.3 ± 0.1^c
Algal growth (nº cell $_x$ 10^5/mL)	4.7 ± 0.4^a	4.1 ± 0.4^a	3.5 ± 0.2^b
Cell volume (μm^3)	20.5 ± 3.8^a	21.0 ± 4.3^a	18.6 ± 3.0^b
Cell length (µm)	9.8 ± 1.8^a	10.0 ± 2.0^a	8.9 ± 1.4^b

Statistics analyzed by Fisher's test are presented as mean ± SD ($p < 0.05$). The letters represent the treatment averages; equal letters indicate equal averages, whereas different letters denote differences between them. mg/100 mg: lipid for every 100 mg of algal biomass wet weight

Photosynthetic pigments content

Photosynthetic pigment kinetics indicated a significant increase in chlorophyll a, b, and total carotenoids levels in *R. subcapitata* in all treatments along the exposure period (192 h) (Fig. 3). However, the photosynthetic pigment content was higher at 2.8 µg/L compared with the control group and the highest concentration (5.6 µg/L). Available evidence suggests that exposure to azole compounds may lead to increased chlorophyll levels, potentially as a compensatory mechanism in response to reactive oxygen species (ROS) formation during energy metabolism (Guo et al., 2020).

Pan et al. (2018) observed an increase in chlorophyll content in *S. obliquus* after exposure for 192 h to the imidazole fungicide climbazole at concentrations ranging from 0.25 to 2 mg/L. Liu et al. (2019) similar results of increased chlorophyll were observed after exposing *C. vulgaris* to low concentrations of paclobutrazol enantiomers (1 mg/L). A reduction in the levels of photosynthetic pigments (chlorophyll a, chlorophyll b, and carotenoids) was identified by Qin et al. (2024) in *A. pyrenoidosa* exposed to cyproconazole, imazalil, and prochloraz after 96 h. In this study, the authors report that chlorophyll content inhibition was positively correlated with growth reduction, likely induced by azole fungicides, resulting in decreased photosynthetic efficiency and algal growth inhibition.

Although it is well established that chlorophyll a is more abundant in photosynthetic organisms, in the present study, the accessory pigments (chlorophyll b and carotenoids) showed the greatest increase. In addition, higher levels

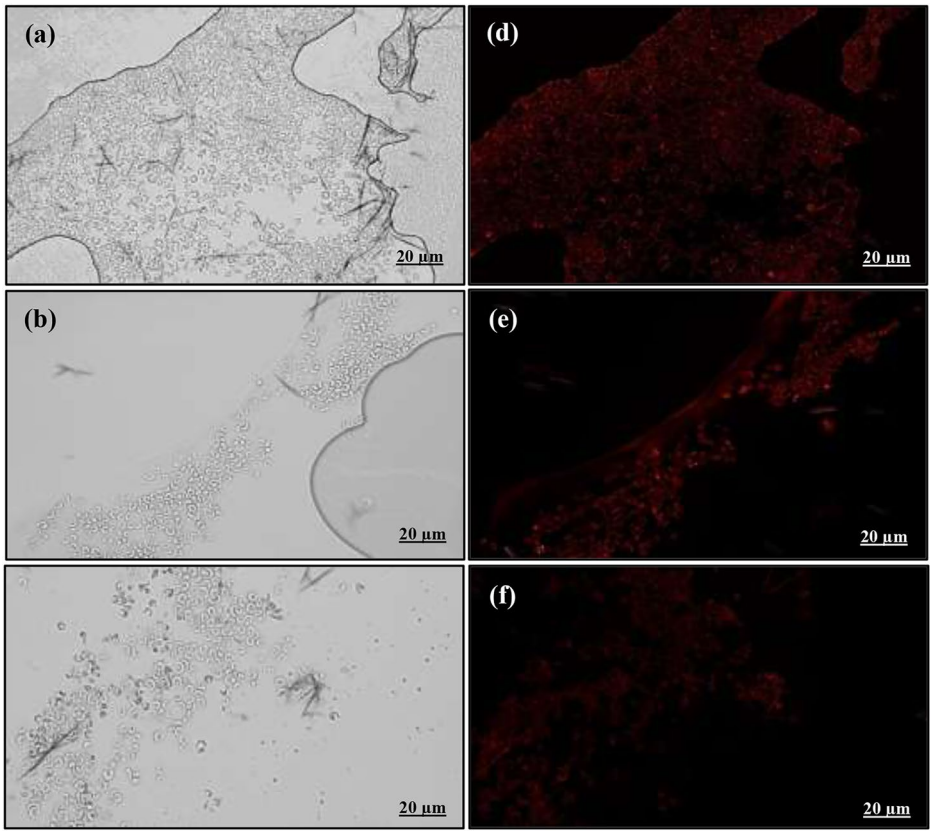


Fig. 2 Microscopic depiction of lipid content in R. subcapitata after 192 h exposure to KTZ. The A-C images show the cell morphology in the background, using the BF method in grayscale with 40x magnification. At the same time, the images of D-F fluorescence microscopy of the lipid content were stained with Nile red dye (0.3 mg/mL) by the UFGW method (50ms), with a magnification of 40x. Grayscale control (a), cells exposed to 2.8 µg/L of KTZ on grayscale (b), cells exposed to 5.6 µg/L of KTZ on grayscale (c), fluorescence microscopy of control cells (d), fluorescence microscopy of cells exposed to 2.8 µg/L of KTZ (e), fluorescence microscopy of cells exposed to 5.6 µg/L of KTZ (f)

of chlorophyll b than chlorophyll a were observed, with values ranging from 0.25 to 0.24 mg/L at 96 h and from 0.60 to 0.50 mg/L at 192 h, respectively. At the end of the test (192 h), chlorophyll b levels were significantly higher than chlorophyll a in all treatments ($p<0.01$). We believe that this is due to possible damage induced by the KTZ, where the oxidation of chlorophyll a (primary photosynthetic pigment) occurs, transforming it into chlorophyll b, a mechanism already observed by Filová et al. (2021) in *R. subcapitata*. Moreover, another important factor is the reduction in cell density in organisms exposed to 5.6 µg/L, which directly affects chlorophyll concentration and pigment analysis relative values, as observed in Table S2.

In addition, natural compounds such as carotenoids have high antioxidant activity by capturing reactive species, also known as non-enzymatic or exogenous antioxidants (Ighodaro and Akinloye 2018). Studies indicate that carotenoids can react with reactive radicals harmful to the physiological system, such as peroxyl radicals (ROO$^{\bullet}$), $^{\bullet}$OH and $O_2^{\bullet}$ (Madkour 2020). As shown in Table 1, the highest KTZ concentration (5.6 µg/L) significantly reduced organism density, which may account for the decrease in photosynthetic pigment content. In contrast, the lower concentration (2.8 µg/L) appears to have a greater capacity to reverse the effects induced by KTZ.

KTZ-induced oxidative stress

Significant changes ($p<0.01$) were observed in all biochemical responses induced by KTZ (Fig. 4) compared to the control group. SOD activity (Fig. 4a) exhibited a significant increase at 96 h (3.8–4.0-fold), followed by a decrease at 192 h (1.1–1.6-fold) for 2.8 and 5.6 µg/L, respectively. LPO levels (Fig. 4b) showed changes only at 192 h, with an average increase of 2.2-fold. In contrast, GST (Fig. 4c) and APx (Fig. 4d) only increased activity at 96 h, with 2.2 and 3.6-fold increases for 2.8 and 5.6 µg/L of KTZ, respectively. Similar to SOD, CAT (Fig. 4e) showed higher activity at 96 h, followed by a reduction in its levels at 192 h, approximately 4.2 and 3.5-fold at 2.8 and 5.6 µg/L, respectively.

The exposure to toxic substances disrupts the homeostasis of living organisms, like the metabolic processes of animals, plants, and photosynthetic organisms, which present phase I and II transformation and detoxification mechanisms (Guo et al. 2020). Phase I represents the action of reductive enzymes, including the CYP complex (monooxygenase enzymes), making toxic molecules more polar (Iacopetta et al. 2023). Phase II involves the action of catalytic enzymes, such as glutathione S-transferase (GST) and N-acetyltransferase (NAT) (Konstandi and Johnson 2023). Studies using fuberidazole (an imidazole fungicide) in *R. subcapitata* after 96 h exhibited changes in biomarker

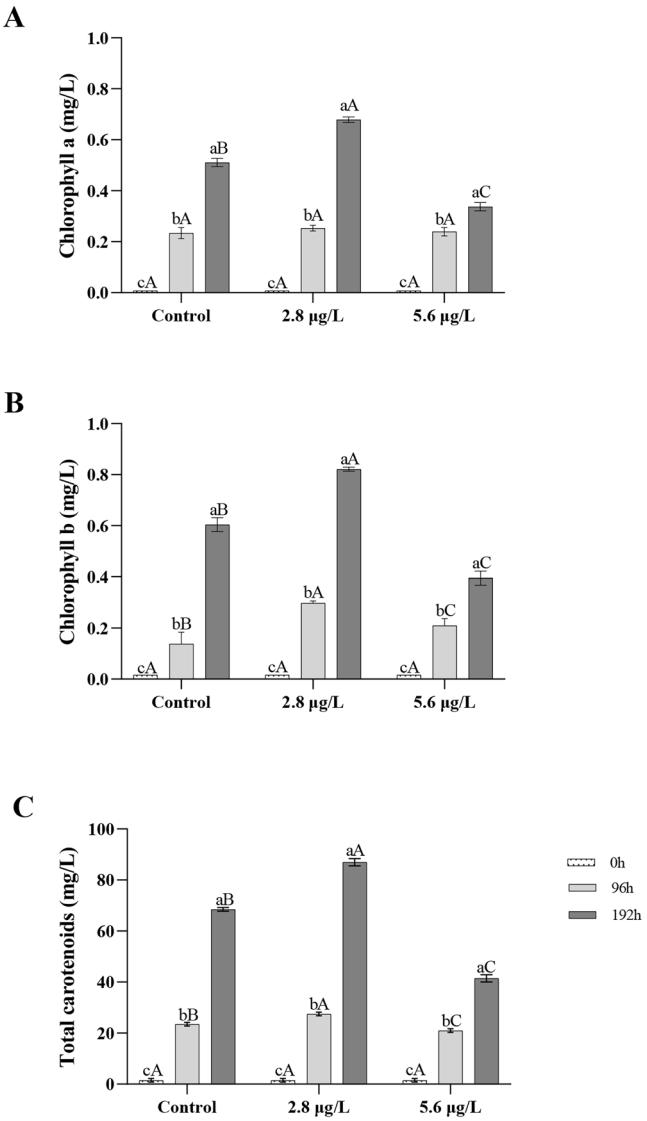


Fig. 3 Analysis of photosynthetic pigment content in *R. subcapitata* over 192 h of exposure to KTZ. Determination of chlorophyll a (a), chlorophyll b (b), and total carotenoids (c). Equal letters indicate no significant difference and different letters indicate a significant difference between the groups (Fisher's LSD test). Lowercase letters represent the responses between different concentrations at the same time point. Capital letters indicate the same treatment over different exposure time points. Data are presented as mean values ± SD ($p < 0.05$)

responses, consistent with oxidative stress-induced damage (Huang et al. 2025). Liu et al. (2019) observed an increase in LPO levels and enzymatic activity (SOD, APx, CAT, and GPx) in *Chlorella vulgaris* after 96 h of exposure to paclobutrazol (a triazole fungicide), similar to the findings in the present study (Fig. 4).

The defense strategies come into play for systemic maintenance, such as first line enzymes, SOD, CAT, APx and GPx (Kaur et al. 2023), which act to neutralize the superoxide radical ($O_2^{\bullet}$), which is highly reactive and harmful to the physiological system. Thus, its conversion into hydrogen peroxide (H_2O_2), followed by its decomposition into water (H_2O) and molecular oxygen (O_2), can regularize the functioning between radicals/redox (García-Caparrós et al. 2021).

The increase in SOD, GST, and APx activities at 96 h is consistent with an enhanced oxidative challenge and activation of antioxidant and detoxification pathways following KTZ exposure (Fig. 4). Despite these responses, the concomitant elevation in LPO levels indicates the occurrence of oxidative damage, suggesting that reactive species production may have partially exceeded the antioxidant capacity (Fig. 4b). CAT exhibited a less consistent pattern, which may reflect enzyme inhibition at higher exposure levels or a functional shift toward APx-mediated H_2O_2 removal. Previous studies report that CAT activity is often associated with elevated H_2O_2 levels in a dose-dependent manner (Ighodaro and Akinloye 2018), whereas APx has a higher affinity for H_2O_2 and contributes to its reduction to water using ascorbate as an electron donor across different subcellular compartments (Li 2023). Overall, the concentration- and time-dependent responses indicate a progressive, sublethal oxidative imbalance and potential disruption of cellular redox homeostasis at environmentally relevant KTZ levels.

According to Liu et al. (2019), an increase in ROS production was observed, possibly leading to increased activity of line I markers, as observed in the present study (Fig. 4). Additionally, while CAT functions in the cytoplasm, APx is capable of removing H_2O_2 in chloroplasts and cytoplasm through the ascorbate–glutathione cycle (ASC-GSH) (Liu et al. 2019; Wang et al. 2023). Studies suggest that the increase in APx in microalgae may be linked to the mechanisms of regulation and elimination of ROS produced during the photoreduction process that occurs in photosynthesis (Ortiz-Espín et al. 2018; Madkour 2020; Ugya et al. 2020; Wang et al. 2023; Zhang et al. 2024). This strategy supports both the protection of the photosynthetic apparatus and the fine regulation of redox signaling (Li 2023). Consistent with this, such a response pattern has been widely reported in plants and green algae (Ortiz-Espín et al. 2018; Li 2023; Lindor et al. 2025). Consistent with these findings, the higher APx activity observed in the present study (Fig. 4d and e) indicates a more pronounced protective role than that of CAT, corroborating trends reported in previous studies.

In addition to antioxidant activity, GST detoxifies xenobiotic molecules, participating in the phase II detoxification pathway (Iacopetta et al.,2023). Its function directly increases the solubility of xenobiotic molecules, simplifying the conjugation process and their eventual excretion (Esteves et al. 2021). Furthermore, high levels of LPO were observed in both KTZ, suggesting possible damage from free radical action on *R. subcapitata* cells (Fig. 4B).

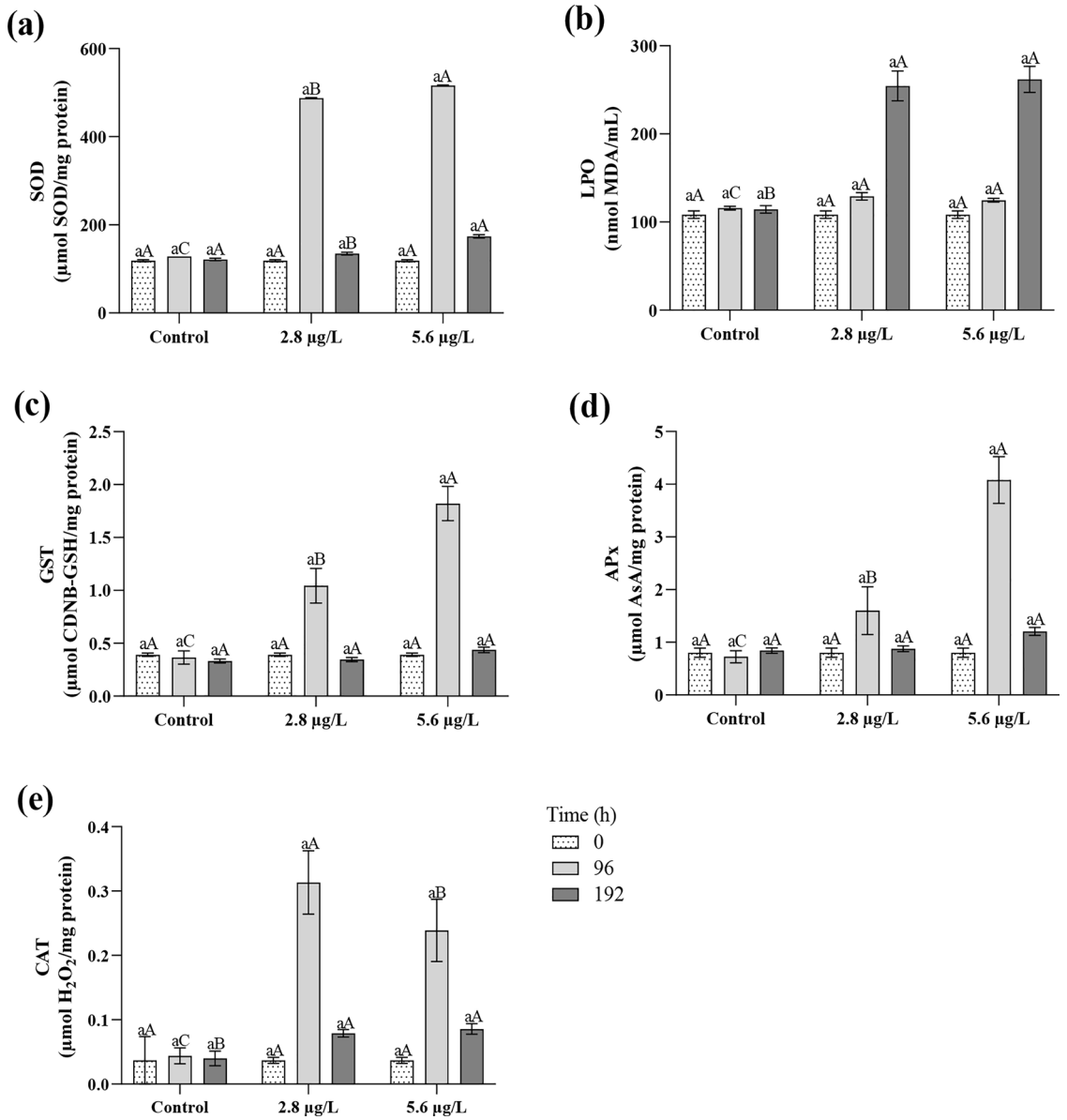


Fig. 4 Biomarkers of oxidative stress in *R. subcapitata* exposure to KTZ. Analysis of SOD (a), LPO (b), GST (c), APx (d), and CAT (e) biomarkers after 0, 96, and 192 h exposure to KTZ. Lowercase letters indicate responses across different concentrations at the same time point. Capital letters indicate the same treatment over different exposure time points. p-value considered significant, $p < 0.01$. The inoculum treatment was used as an internal control for the assays (0 h). Data are presented as mean values ± SEM (standard error of the mean)

Comparing the production of photosynthetic pigments and antioxidant activity, it is possible to observe an inversely proportional response, in which the treatment with the lowest concentration of KTZ (2.8 µg/L) showed the highest production of pigments (Fig. 3) while showing low enzymatic activity (Fig. 4). However, it was observed that the treatment and higher concentration (5.6 µg/L) demanded more significant enzymatic activity, which may be related to the reduction in pigment production since they also function as non-enzymatic antioxidants.

Multivariate analysis

Principal component analysis (PCA) provided a comprehensive overview of the multivariate response of *R. subcapitata* to KTZ exposure, explaining 78.62% of the total variance through the first two components (PC1 = 48.37%, PC2 = 30.25%) (Fig. 5) (Table S3). The distribution of treatment groups and the orientation of the vectors representing biological and physiological variables revealed distinct response patterns, indicating time-dependent toxicological effects.

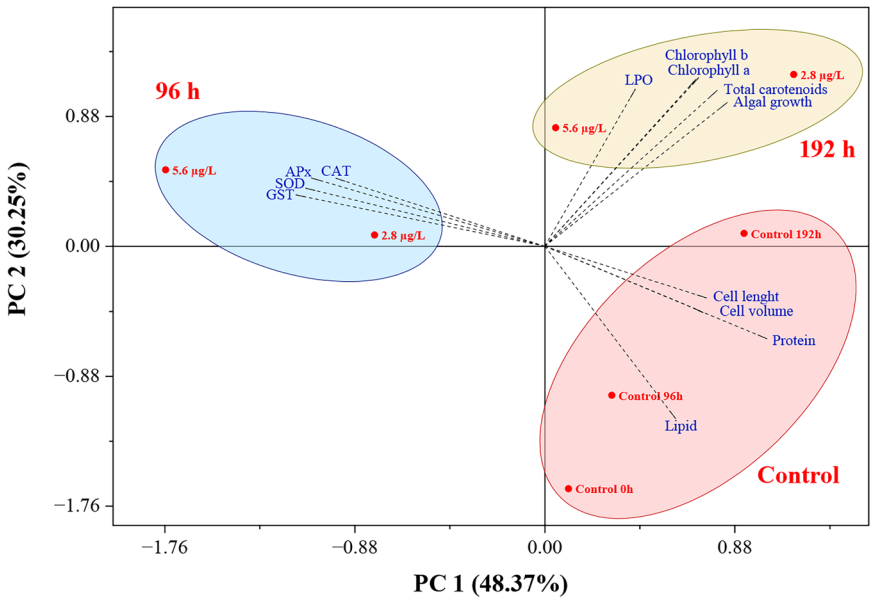


Fig. 5 Principal component analysis (PCA) in Raphidocelis. subcapitata after exposure to KTZ

The control groups (0 h, 96 h, and 192 h) clustered together on the right side of the biplot (red ellipse), strongly associated with variables such as cell length, cell volume, lipid, and protein content. These variables are typically associated with normal physiological status, suggesting that the absence of the contaminant enabled the algae to maintain cellular integrity and metabolic stability throughout the experiment. In contrast, exposure to KTZ at 96 h resulted in a markedly different profile (blue ellipse), characterized by increased activity of antioxidant enzymes, including SOD, CAT, APx, and GST. This grouping reflects a clear oxidative stress response, indicating that higher concentrations of KTZ induce cellular damage and activate defense mechanisms that neutralize reactive oxygen species (ROS). After 192 h exposure, the variables associated with photosynthetic activity, including chlorophyll a, chlorophyll b, carotenoids, and algal growth rate, were more representative (yellow ellipse).

SOD and APx exhibited the highest activity in response to KTZ. The decrease in lipid levels may be related to the increase in lipid peroxidation observed (Fig. 4b). Likewise, the increase in photosynthetic pigment content may be related to the rise in APx activity at the highest KTZ concentration (Figs. 3 and 4d). Thus, we believe that the mechanisms related to the redox balance for *R. subcapitata* are related not only to the induction of the endogenous antioxidant system but also to the biosynthesis of protective pigments, as already observed in several studies (Ortiz-Espín et al. 2018; Pan et al. 2018; Liu et al. 2019; Guo et al. 2020; Xiang et al. 2023; Zhang et al. 2024; Qin et al. 2024).

Overall, the PCA demonstrates a time-dependent bifurcation in the algal response. While longer exposure times may enhance photosynthetic performance, shorter exposure times may temporarily activate stress-response pathways and compromise cellular function. These temporal variations underscore the importance of considering both stimulatory effects, such as the transient enhancement of photosynthetic-related parameters, and inhibitory effects, particularly during the early activation of stress-response pathways at shorter exposure times, when evaluating the risks of environmentally relevant concentrations of KTZ in aquatic environments. Indeed, we acknowledge that establishing a robust mechanistic understanding of KTZ toxicity based on only three sampling points (0, 96, and 192 h) may limit the ability to fully interpret these responses. Nevertheless, given the current lack of information regarding the effects of KTZ on photosynthetic organisms, the results presented here may provide valuable baseline data and serve as a relevant reference for future studies.

Conclusion

This study demonstrates the sensitivity of the freshwater microalgae *R. subcapitata* to environmentally relevant concentrations of the commercial KTZ formulation. The IC_{50} was determined at 7.2 µg/L. Additionally, KTZ exhibits concentration- and time-dependent effects on the alga. Low concentrations (2.8 µg/L) were associated with increased photosynthetic pigment content and growth, suggesting a transient stimulation of photosynthetic pigments. However, higher concentrations (5.6 µg/L) result in oxidative stress, as evidenced by the activation of antioxidant enzymes (SOD, CAT, APx, and GST), indicating a disruption of cellular homeostasis. The high concentration also reduced lipid storage and morphological variables, such as cell volume

and length. Overall, our findings underscore the ecological risk associated with subinhibitory exposure to commercial KTZ formulations, which can significantly alter algal physiology. In this context, our results highlight the importance of incorporating time-dependent, ecotoxicologically relevant suborganismic biomarkers, together with biochemical and morphological endpoints, alongside traditional apical endpoints in environmental risk assessment. Accounting for these early, mechanistically informative responses can improve the detection of subtle but ecologically meaningful effects of pharmaceutical contaminants, thereby strengthening monitoring strategies and supporting more protective regulatory frameworks for aquatic ecosystems.

Supplementary Information The online version contains supplementary material available at https://doi.org/10.1007/s10646-026-03066-z.

Acknowledgements We would like to thank the Coordenação de Aperfeiçoamento de Pessoa de Nível Superior – Brasil (CAPES) (Finance code 001).

Author contributions C.C.A.Prado: Conceptualization, Methodology, Formal analysis, Data curation, Investigation, Visualization, Writing – original draft, Writing – review and editing. L.G.Queiroz: Formal analysis, Data curation, Investigation, Visualization, Writing – original draft, Writing – review and editing. F.T.Silva: Supervision, Writing – review and editing, Funding acquisition. T.C.B.Paiva: Supervision, Writing – review and editing, Funding acquisition.

Funding The Article Processing Charge (APC) for the publication of this research was funded by the Coordenação de Aperfeiçoamento de Pessoal de Nível Superior - Brasil (CAPES) (ROR identifier: 00x0ma614).

Data availability No datasets were generated or analysed during the current study.

Declarations

Conflict of interest The authors declare no competing interests.

Open Access This article is licensed under a Creative Commons Attribution 4.0 International License, which permits use, sharing, adaptation, distribution and reproduction in any medium or format, as long as you give appropriate credit to the original author(s) and the source, provide a link to the Creative Commons licence, and indicate if changes were made. The images or other third party material in this article are included in the article's Creative Commons licence, unless indicated otherwise in a credit line to the material. If material is not included in the article's Creative Commons licence and your intended use is not permitted by statutory regulation or exceeds the permitted use, you will need to obtain permission directly from the copyright holder. To view a copy of this licence, visit http://creativecommons.org/licenses/by/4.0/.

References

ABNT 12648 (2018) Ecotoxicologia aquática - Toxicidade crônica - Método de ensaio com algas (Chlophyceae) - ABNT NBR 12648. Associação Brasileira de Normas Técnicas 2o edição:1–33

Assress HA, Nyoni H, Mamba BB, Msagati TAM (2020) Occurrence and risk assessment of azole antifungal drugs in water and wastewater. Ecotoxicol Environ Saf 187:109868. https://doi.org/10.1016/j.ecoenv.2019.109868

Batucan NSP, Tremblay LA, Northcott GL, Matthaei CD (2022) Medicating the environment? A critical review on the risks of carbamazepine, diclofenac and ibuprofen to aquatic organisms. Environmental advances, 7, 100164. https://doi.org/10.1016/j.envadv.2021.100164

Bhagat J, Singh N, Nishimura N, Shimada Y (2021) A comprehensive review on environmental toxicity of azole compounds to fish. Chemosphere 262:128335. https://doi.org/10.1016/j.chemosphere.2020.128335

Bradford MM (1976) A rapid and sensitive method for the quantitation of microgram quantities of protein utilizing the principle of protein-dye binding. Anal Biochem 254:248–254. https://doi.org/10.1016/0003-2697(76)90527-3

Chaves M, de JS, Barbosa SC, de Malinowski M M, et al (2020) Pharmaceuticals and personal care products in a Brazilian wetland of international importance: Occurrence and environmental risk assessment. Sci Total Environ 734:139374. https://doi.org/10.1016/j.scitotenv.2020.139374

Chen ZF, Ying GG (2015) Occurrence, fate and ecological risk of five typical azole fungicides as therapeutic and personal care products in the environment: A review. Environ Int 84:142–153. https://doi.org/10.1016/j.envint.2015.07.022

Chen Z-F, Ying G-G, Jiang Y-X et al (2014) Photodegradation of the azole fungicide fluconazole in aqueous solution under UV-254: Kinetics, mechanistic investigations and toxicity evaluation. Water Res 52:83–91. https://doi.org/10.1016/j.watres.2013.12.039

Dehm J, Singh S, Ferreira M et al (2021) Screening of pharmaceuticals in coastal waters of the southern coast of Viti Levu in Fiji, South Pacific. Chemosphere 276:130161. https://doi.org/10.1016/j.chemosphere.2021.130161

Del Puerto O, Gonçalves NPF, Medana C et al (2022) Attenuation of toxicity and occurrence of degradation products of the fungicide tebuconazole after combined vacuum UV and UVC treatment of drinking water. Environ Sci Pollut Res 29:58312–58325. https://doi.org/10.1007/s11356-022-19691-0

Esteves F, Rueff J, Kranendonk M (2021) The Central Role of Cytochrome P450 in Xenobiotic Metabolism — A Brief Review on a Fascinating Enzyme Family. J Xenobiot 11:94–114

Filová A, Fargašová A, Molnárová M (2021) Cu, Ni, and Zn effects on basic physiological and stress parameters of Raphidocelis subcapitata algae. Environ Sci Pollut Res 28:58426–58441. https://doi.org/10.1007/s11356-021-14778-6

Fu L, Huang T, Wang S et al (2017) Toxicity of 13 different antibiotics towards freshwater green algae Pseudokirchneriella subcapitata and their modes of action. Chemosphere 168:217–222. https://doi.org/10.1016/j.chemosphere.2016.10.043

García-Caparrós P, De Filippis L, Gul A et al (2021) Oxidative Stress and Antioxidant Metabolism under Adverse Environmental Conditions: a Review. Bot Rev 87:421–466. https://doi.org/10.1007/s12229-020-09231-1

Gonçalves NPF, del Puerto O, Medana C et al (2021) Degradation of the antifungal pharmaceutical clotrimazole by UVC and vacuum-UV irradiation: Kinetics, transformation products and attenuation of toxicity. J Environ Chem Eng 9:106275. https://doi.org/10.1016/j.jece.2021.106275

Grycová A, Dořičáková A, Dvořák Z (2015) Impurities contained in antifungal drug ketoconazole are potent activators of human aryl hydrocarbon receptor. Toxicol Lett 239:67–72. https://doi.org/10.1016/j.toxlet.2015.09.004

Guo J, Peng J, Lei Y et al (2020) Comparison of oxidative stress induced by clarithromycin in two freshwater microalgae Raphidocelis subcapitata and Chlorella vulgaris. Aquat Toxicol 219:105376. https://doi.org/10.1016/j.aquatox.2019.105376

Hannas BR, Wang YH, Thomson S et al (2011) Regulation and dysregulation of vitellogenin mRNA accumulation in daphnids (Daphnia magna). Aquat Toxicol 101:351–357. https://doi.org/10.1016/j.aquatox.2010.11.006

Huang Y, Guo D, Qin L et al (2025) Toxic effects of eight azole fungicides on the growth, photosynthetic activity, and oxidative stress of *Raphidocelis subcapitata*. Environ Toxicol Chem 44:1259–1271. https://doi.org/10.1093/etojnl/vgaf003

Hussain A, Alshehri S, Ramzan M et al (2021) Biocompatible solvent selection based on thermodynamic and computational solubility models, in-silico GastroPlus prediction, and cellular studies of ketoconazole for subcutaneous delivery. J Drug Deliv Sci Technol 65:102699. https://doi.org/10.1016/j.jddst.2021.102699

Iacopetta D, Ceramella J, Catalano A et al (2023) Impact of Cytochrome P450 Enzymes on the Phase I Metabolism of Drugs. Appl Sci 13:6045. https://doi.org/10.3390/app13106045

Iancu V-I, Chiriac L-F, Paun I et al (2024) Occurrence and distribution of azole antifungal agents in eight urban Romanian waste water treatment plants. Sci Total Environ 920:170898. https://doi.org/10.1016/j.scitotenv.2024.170898

Ighodaro OM, Akinloye OA (2018) First line defence antioxidants-superoxide dismutase (SOD), catalase (CAT) and glutathione peroxidase (GPX): Their fundamental role in the entire antioxidant defence grid. Alexandria J Med 54:287–293. https://doi.org/10.1016/j.ajme.2017.09.001

Jesus SS, Ferreira GF, Moreira LS et al (2019) Comparison of several methods for effective lipid extraction from wet microalgae using green solvents. Renew Energy 143:130–141. https://doi.org/10.1016/j.renene.2019.04.168

Kaur M, Bhatia S, Sangha MK, Phutela UG (2023) Crosstalk of AsA/DHA and GSH/GSSG ratios' role in growth-phase dependent antioxidative defense in euryhaline and freshwater microalgae: explored for the first time. Physiol Mol Biology Plants 29:1457–1474. https://doi.org/10.1007/s12298-023-01349-x

Konstandi M, Johnson EO (2023) Age-related modifications in CYP-dependent drug metabolism: role of stress. Front Endocrinol (Lausanne) 14. https://doi.org/10.3389/fendo.2023.1143835

Li S (2023) Novel insight into functions of ascorbate peroxidase in higher plants: More than a simple antioxidant enzyme. Redox Biol 64:102789. https://doi.org/10.1016/j.redox.2023.102789

Lindor A, Castro MS, Guimarães PS et al (2025) Sensitivity of two green microalgae to clomazone: insights into oxidative stress and defense systems. Ecotoxicology 34:2131–2139. https://doi.org/10.1007/s10646-025-02978-6

Liu C, Liu S, Diao J (2019) Enantioselective growth inhibition of the green algae (Chlorella vulgaris) induced by two paclobutrazol enantiomers. Environ Pollut 250:610–617. https://doi.org/10.1016/j.envpol.2019.04.027

Madkour LH (2020) Nanoparticles Induce Oxidative and Endoplasmic Reticulum Stresses. Springer International Publishing, Cham

Maraqa MA, Meetani M, Alhalabi AM (2020) Effectiveness of conventional wastewater treatment processes in removing pharmaceutically active compounds. IOP Conf Ser Earth Environ Sci 424. https://doi.org/10.1088/1755-1315/424/1/012014

Miazek K, Brozek-Pluska B (2019) Effect of PHRs and PCPs on Microalgal Growth, Metabolism and Microalgae-Based Bioremediation Processes: A Review. Int J Mol Sci 20:2492. https://doi.org/10.3390/ijms20102492

Morais SA, Delerue-Matos C, Gabarrell X (2014) An uncertainty and sensitivity analysis applied to the prioritisation of pharmaceuticals as surface water contaminants from wastewater treatment plant direct emissions. Sci Total Environ 490:342–350. https://doi.org/10.1016/j.scitotenv.2014.04.082

Nong QY, Liu YA, Qin LT et al (2021) Toxic mechanism of three azole fungicides and their mixture to green alga Chlorella pyrenoidosa. Chemosphere 262:127793. https://doi.org/10.1016/j.chemosphere.2020.127793

OECD 201 (2011) Test No. 201: Freshwater Alga and Cyanobacteria, Growth Inhibition Test. Guidelines for the Testing of Chemicals, OECD 1–25. https://doi.org/10.1145/1294046.1294048

Ortiz-Espín A, Sánchez-Guerrero A, Sevilla F, Iménez A (2018) Ascorbic Acid in Plant Growth, Development and Stress Tolerance. In: Ascorbic Acid in Plant Growth, Development and Stress Tolerance. pp 1–511

Pan C-G, Peng F-J, Ying G-G (2018) Removal, biotransformation and toxicity variations of climbazole by freshwater algae Scenedesmus obliquus. Environ Pollut 240:534–540. https://doi.org/10.1016/j.envpol.2018.05.020

Peng X, Huang Q, Zhang K et al (2012) Distribution, behavior and fate of azole antifungals during mechanical, biological, and chemical treatments in sewage treatment plants in China. Sci Total Environ 426:311–317. https://doi.org/10.1016/j.scitotenv.2012.03.067

Porsbring T, Blanck H, Tjellström H, Backhaus T (2009) Toxicity of the pharmaceutical clotrimazole to marine microalgal communities. Aquat Toxicol 91:203–211. https://doi.org/10.1016/j.aquatox.2008.11.003

Prado CCA, Queiroz LG, Silva FT, Paiva TCB (2021) Ecotoxicological effect of ketoconazole on the antioxidant system of Daphnia similis. Comp Biochem Physiol C: Toxicol Pharmacol 246:109080. https://doi.org/10.1016/j.cbpc.2021.109080

Prado CCA do, Queiroz LG, da Silva FT, de Paiva TCB (2023) Toxicological effects caused by environmental relevant concentrations of ketoconazole in Chironomus sancticaroli (Diptera, Chironomidae) larvae evaluated by oxidative stress biomarkers. Comp Biochem Physiol C: Toxicol Pharmacol 264:109532. https://doi.org/10.1016/j.cbpc.2022.109532

Priyanka P, Kinsella GK, Henehan GT, Ryan B (2020) Nile Red assay development for the estimation of neutral lipids in *Chlorella emersonii* and *Pseudokirchneriella subcapitata*. Eurobiotech J 4:216–222. https://doi.org/10.2478/ebtj-2020-0025

Qin L-T, Lei Y-X, Liu M et al (2024) Toxic interactions at the physiological and biochemical levels of green algae under stress of mixtures of three azole fungicides. Sci Total Environ 926:171771. https://doi.org/10.1016/j.scitotenv.2024.171771

Rubim AM, dos Santos MR, Laporta LVJ et al (2012) Quantitative determination of ketoconazole tablets by absorption spectrophotometry in the ultraviolet region. Rev Bras Farm 93:510–514

Sadozai SK, Khan SA, Karim N et al (2020) Ketoconazole-loaded PLGA nanoparticles and their synergism against Candida albicans when combined with silver nanoparticles. J Drug Deliv Sci Technol 56:101574. https://doi.org/10.1016/j.jddst.2020.101574

Shafiei M, Peyton L, Hashemzadeh M, Foroumadi A (2020) History of the development of antifungal azoles: A review on structures, SAR, and mechanism of action. Bioorg Chem 104:104240. https://doi.org/10.1016/j.bioorg.2020.104240

Skalska-Tuomi K, Kaijanen L, Monteagudo JM, Mänttäri M (2025) Efficient removal of pharmaceuticals from wastewater: Comparative study of three advanced oxidation processes. J Environ Manage 375:124276. https://doi.org/10.1016/j.jenvman.2025.124276

Styszko K, Bolesta W, Worek J et al (2025) Tracking nonregulated micropollutants in sewage sludge: Antimicrobials, OH-PAHs, and microplastics — Environmental risks, fertilizer implications and energy considerations. Energy Rep 13:4756–4768. https://doi.org/10.1016/j.egyr.2025.04.013

Ugya AY, Imam TS, Li A et al (2020) Antioxidant response mechanism of freshwater microalgae species to reactive oxygen species production: a mini review. Chem Ecol 36:174–193. https://doi.org/10.1080/02757540.2019.1688308

Villain J, Minguez L, Halm-Lemeille M-P et al (2016) Acute toxicities of pharmaceuticals toward green algae. mode of action, biopharmaceutical drug disposition classification system and quantile regression models. Ecotoxicol Environ Saf 124:337–343. https://doi.org/10.1016/j.ecoenv.2015.11.009

Volkman J (2003) Sterols in microorganisms. Appl Microbiol Biotechnol 60:495–506. https://doi.org/10.1007/s00253-002-1172-8

Voshall A, Christie NTM, Rose SL et al (2021) Sterol Biosynthesis in Four Green Algae: A Bioinformatic Analysis of the Ergosterol Versus Phytosterol Decision Point. J Phycol 57:1199–1211. https://doi.org/10.1111/jpy.13164

Wang L, Yang T, Pan Y et al (2023) The Metabolism of Reactive Oxygen Species and Their Effects on Lipid Biosynthesis of Microalgae. Int J Mol Sci 24:11041. https://doi.org/10.3390/ijms241311041

Wattanayon R, Proctor K, Jagadeesan K et al (2023) An integrated One Health framework for holistic evaluation of risks from antifungal agents in a large-scale multi-city study. Sci Total Environ 900:165752. https://doi.org/10.1016/j.scitotenv.2023.165752

Wroński M, Trawiński J, Skibiński R (2024) Antifungal drugs in the aquatic environment: A review on sources, occurrence, toxicity, health effects, removal strategies and future challenges. J Hazard Mater 465:133167. https://doi.org/10.1016/j.jhazmat.2023.133167

Xiang Q, Zhou Y, Tan C (2023) Enantioselective Toxic Effects of Prothioconazole toward Scenedesmus obliquus. Molecules 28:4774. https://doi.org/10.3390/molecules28124774

Yamagishi T, Horie Y, Tatarazako N (2017) Synergism between macrolide antibiotics and the azole fungicide ketoconazole in growth inhibition testing of the green alga Pseudokirchneriella subcapitata. Chemosphere 174:1–7. https://doi.org/10.1016/j.chemosphere.2017.01.071

Yang Z, Guo F, Bunn SE et al (2025) Resource Quality and Quantity Exert Distinct Influences on Trophic Interactions and Food Web Pyramids Under Different Nutrient Conditions. https://doi.org/10.1111/fwb.70073. Freshw Biol 70:

Yousefi-Ahmadipour A, Bozorgi-Koshalshahi M, Mogharabi M et al (2016) Laccase-catalyzed treatment of ketoconazole, identification of biotransformed metabolites, determination of kinetic parameters, and evaluation of micro-toxicity. J Mol Catal B Enzym 133:77–84. https://doi.org/10.1016/j.molcatb.2016.07.015

Zhang Y, Sun D, Gao W et al (2024) The metabolic mechanisms of Cd-induced hormesis in photosynthetic microalgae, Chromochloris zofingiensis. Sci Total Environ 912:168966. https://doi.org/10.1016/j.scitotenv.2023.168966

Publisher's note Springer Nature remains neutral with regard to jurisdictional claims in published maps and institutional affiliations.